Proceedings of ASME Turbo Expo 2011
GT2011
June 6-10, 2011, Vancouver, British Columbia, Canada

GT2011-45626

POWER RESERVE CONTROL FOR GAS TURBINES IN COMBINED CYCLE APPLICATIONS

Eric A. Müller, Andrew Wihler
Alstom Power
Baden, Switzerland

ABSTRACT

In order to be able to optimally operate a combined cycle power plant in a liberalized electricity market, knowledge of the plant's maximum exportable power generation capacity is vital. However, the maximum power output of a power plant is affected by numerous variable factors, such as the ambient conditions at the plant site. In addition, the allowable plant operating range might be narrowed by a compulsory reserve margin, if the power plant is participating in a frequency regulation program. In this paper, a power reserve controller is derived, which facilitates the optimal operation of a combined cycle gas turbine power plant subject to a reserve margin requirement. The power reserve controller bases on a mathematical description of the power plant and uses an adaptation mechanism to predict on a real-time basis the maximum allowable plant load limit. Based on tests on a single shaft combined cycle power plant, the operation of the power reserve controller is demonstrated and its performance is assessed. The test results prove that the controller predicts the maximum power output of the plant with high accuracy and that it is able to maintain a desired reserve capacity for frequency response as specified.

INTRODUCTION

In order to supply energy to an electrical grid, all connected power generators are obliged to comply with the grid code of the local transmission system. An integral part of modern transmission system grid codes is the functional description of frequency support services. The objective of an active frequency control is the limitation of grid frequency excursions by an automatic adjustment of the generated power. Frequency support cannot be provided if a power generator is dispatched at its operating limit. For this reason, some grid codes explicitly specify a minimum power capacity, which a power generator has to maintain in reserve for frequency support (see for example [1–5]). The power producer, however, typically aims at a maximum generation of its plant for commercial reasons.

An output maximization subject to the power reserve requirement is possible if information about the current upper operating limit of the plant is available. As a matter of fact, the maximum power generation capacity of a combined cycle power plant is generally not precisely known. It is dependent on the ambient conditions at the power plant site (e.g. ambient temperature or pressure) and other variable factors influencing the performance of the individual components, such as heat soaking, dirt accumulation or aging.

Today, a number of different approaches exist to operate a combined cycle power plant such that a desired power generation capacity is maintained in reserve. One class of methods determines the maximum power output based on correction curves and/or occasional calibration when the unit is at maximum load. From the estimated maximum power output the desired reserve capacity is then subtracted in order to yield a load limiting reference value. By definition, the estimated maximum power cannot be corrected for unknown disturbances on a continuous basis with these methods. As a consequence, it cannot be guaranteed that the specified reserve capacity is available when required, unless a conservative safety margin is applied.

Other methods take a specific process quantity (e.g. the angle of the variable guide vanes of the gas turbine compressor) as

indicator of the actual reserve capacity and control it to a precalculated reference value. Since such controllers operate parallel to the standard load control, variations in the manual load set-point and frequency control actions are asymptotically canceled by these controllers. Hence, with such methods, the gas turbine generator cannot be operated at a settable load while the reserve capacity controller is active, nor can long-term frequency support be provided.

The objective of this article is to present a method to control a power reserve margin of a combined cycle power plant, which avoids the shortcomings of the previous methods. The power reserve controller developed operates on the control-hierarchic level of load commands and consists of two separate modules: (i) a module that predicts the maximum power output under the prevailing operating and ambient conditions; and, (ii) a module that determines the power margin that is required in order to maintain the specified reserve capacity for frequency support. The first module has an observer-like structure and estimates on a real-time basis the power plant's maximum generation capacity. The estimation method is based on a mathematical model of the system and uses process measurements to continuously update the model prediction. In the second module, dynamic system properties are factored in, in order to translate the specified reserve capacity for frequency support into load limits. The power reserve controller can handle independent reserve capacities for primary frequency response and secondary frequency regulation.

In the course of the development project, distinct implementations of the power reserve controller were engineered for different combined cycle arrangements (i.e. single shaft, multi-shaft 2 on 1, multi-shaft 1 on 1). Further, a variety of configurations were adopted in order to fulfill different grid code requirements and satisfy special customer needs. A comprehensive discussion of the power reserve controller in all its facets would be beyond the scope of this paper. Therefore, the text at hand focuses on the implementation for the typical arrangement, which is the single shaft power train, and to primary frequency response and primary reserve control, respectively.

In the first part of the paper, a generic introduction to the load control of combined cycle power plants is given as a basis for the later discussion. Subsequently, the definition of a power reserve is introduced. The derivation of the mathematical system model is subject of the next section. The model equations, which were calibrated and experimentally validated with plant data, describe the power dynamics of the combined cycle system. In the following part of the paper, the concept of the power reserve controller is developed and the integration into the load control system is shown. The experimental validation of the power reserve controller's functionality and performance is discussed in a subsequent section. Lastly, the main findings are summarized and the conclusions are drawn.

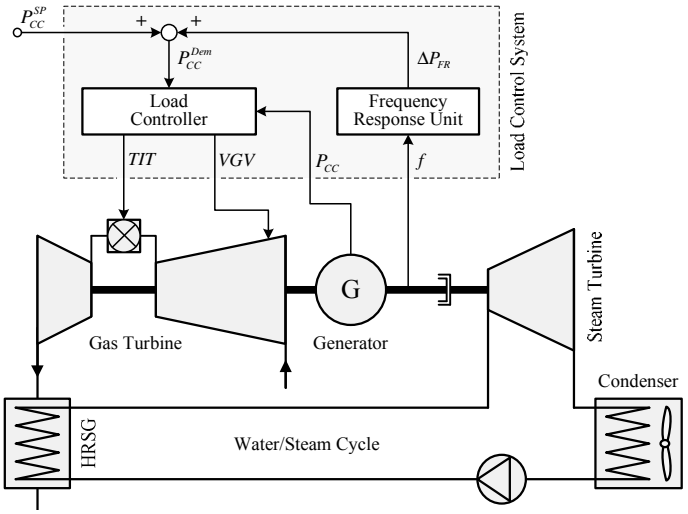

FIGURE 1. SCHEMATIC OF A COMBINED CYCLE GAS TURBINE POWER PLANT WITH LOAD CONTROL SYSTEM.

COMBINED CYCLE POWER PLANTS

The power reserve controller that is described in this paper was first implemented and validated in 2008 at a combined cycle power plant in Italy. The respective plant consists of two Alstom KA26-1 combined cycle power blocks. Each block is comprised of one GT26 gas turbine and a STF15C steam turbine module in a single shaft arrangement. The blocks are gas fired and equipped with hydrogen-cooled TOPGAS turbo generators, three-pressure-level heat recovery steam generators (HRSGs), and air-cooled condensers. The blocks produce a site rated electrical power output of 400 MW each. (For a more detailed product description, see for example [6, 7].)

A schematic of a combined cycle gas turbine power plant is shown in Fig. 1. The gas turbine is employed as prime mover that converts chemical energy of gaseous or liquid fuel into mechanical energy, exhaust enthalpy, and waste heat. The flue gas of the gas turbine is transported through an HRSG, where the exhaust enthalpy is used to produce steam, which is subsequently expanded in the steam turbine in order to generate additional mechanical power. In single shaft configurations, a gas turbine and a steam turbine are coupled to one generator, which converts the mechanical into electrical power.

The power output of the generator is regulated by a control system. The controller enables frequency response operation and ensures that the desired load set-point is followed and maintained. To this end, rotor frequency, f, and active power, P_{CC}, are measured and processed in the frequency response unit and in the load controller, respectively. In the frequency response unit, a regulating power ΔP_{FR} is determined according to the fol-

lowing definition:

$$\Delta P_{FR} = -K_{FR} \cdot \Delta f = -K_{FR} \cdot (f - f_{Ref}) \quad (1)$$

where f_{Ref} is the reference grid frequency and K_{FR} is the frequency-to-power gain of the frequency control system. At the input of the load controller, this power variation for frequency response is added to the load set-point, P_{CC}^{SP}, (i.e., the load at which the power plant is dispatched) in order to yield the overall load demand, P_{CC}^{Dem}.

$$P_{CC}^{Dem} = P_{CC}^{SP} + \Delta P_{FR} \quad (2)$$

In the upper load range, which is the relevant range for the application at hand, the steam turbine is usually operated in sliding pressure mode. In this operating mode, the steam inlet control valves are wide open and the steam turbine power output is determined by the actual operating conditions of the gas turbine. Hence, varying the gas turbine's operating point enables the adjustment of the power output of the combined cycle plant. The operating point of the gas turbine is mainly determined by the position of the variable guide vanes, *VGV*, on the one hand and the value of the mixed turbine inlet temperature, *TIT*, on the other hand.[1] Both *VGV* and *TIT* are outputs of the load controller. The former actuator modulates the mass flow through compressor and turbine, whereas the latter correlates to the amount of fuel injected into the combustion system.

POWER RESERVE SPECIFICATION

If the operating range of a power generator shall include a band which is exclusively reserved for frequency regulation, a corresponding rule is stated in the grid code. Such a power reserve specification usually includes a static requirement as well as a requirement regarding the maximum allowable response time. In Appendix 15 of the Italian Grid Code, for example, the primary reserve is specified as follows [3]:

$\Delta P_{PR} = 0.015 \cdot P_{Eff}$;
50% of ΔP_{PR} to be available within 15 s;
100% of ΔP_{PR} to be available within 30 s; and
ΔP_{PR} to be maintained for at least 15 min,

where ΔP_{PR} is the required reserve capacity and P_{Eff} is the effective power of the unit under ISO conditions. Similar requirements regarding a primary power reserve are formulated in the French Grid Code [4, 5].

For the derivation of the power reserve controller, however, the definition of the reserve capacity was simplified. In fact, the controller was developed based on the following specification:

The power reserve controller shall constrain the load range of the plant such that a power capacity of ΔP_{PR} [MW] *is maintained and available within* Δt_{PR} [s] *for primary frequency response.*

MATHEMATICAL MODEL OF THE SYSTEM

In this section, the equations of the mathematical model are described. The mathematical model presented here is a concise, nonlinear, and time-invariant description of the system's power dynamics. The model was derived based on physical reasoning on the one hand and from correlation analyses on the other hand.

Model Equations

On plant level, the power output comprises a contribution of the gas turbine and a contribution of the steam turbine. Accordingly, the contributions of the two components to the overall power output are considered separately in the model.

For the net quasi-static power output of the gas turbine, $P_{GT}^{qs,mbe}$, the following multiplicative structure is applied:

$$P_{GT}^{qs,mbe} = \gamma_{TK1}(TK1) \cdot P_{GT}^{Nom} \cdot \left[\gamma_{VGV}(VGV) \cdot \gamma_{TIT}(TIT)\right]. \quad (3)$$

The factors $\gamma_{VGV}(VGV)$ and $\gamma_{TIT}(TIT)$ model the variation of the gas turbine power output as functions of the commanded positions of the variable guide vanes and of the mixed turbine inlet temperature, respectively.[2] With the factor $\gamma_{TK1}(TK1)$, the power output is corrected for changing compressor inlet temperatures, *TK1*. All the three factors employed in Eqn. (3) are polynomial functions and satisfy the relation

$$\gamma_{TK1}(TK1_{Nom}) = \gamma_{VGV}(VGV_{Nom}) = \gamma_{TIT}(TIT_{Nom}) = 1. \quad (4)$$

The parameter set $\{TK1_{Nom}, VGV_{Nom}, TIT_{Nom}\}$ defines the reference point of the model with a corresponding power output of P_{GT}^{Nom}. For the application at hand, the model should achieve its highest accuracy in the upper load range. Accordingly, the reference point of the model was chosen to be the nominal operating point of the engine. Further, the polynomial coefficients of the functions γ_{VGV} and γ_{TIT} vary with the compressor inlet temperature and depend on the type of fuel used, i.e., are different for fuel gas operation and fuel oil operation.

[1] In a sequential combustion engine, two distinct mixed turbine inlet temperatures are distinguished.

[2] In the case of a sequential combustion engine, *TIT* shall be representative for the mixed inlet temperature of the low pressure turbine.

In practice, the power response of the gas turbine is delayed with respect to the command at the load controller. In order to consider this dynamic lag, the quasi-static relation of Eqn. (3) was augmented with a first-order dynamic element of time-constant τ_{GT},

$$\Sigma_{GT}(s) = \frac{1}{\tau_{GT} \cdot s + 1} \tag{5}$$

to obtain the estimation of the actual gas turbine power output as

$$P_{GT}^{mbe} = \Sigma_{GT}(s) \cdot P_{GT}^{qs,mbe}. \tag{6}$$

The power output of the steam turbine depends on the exhaust enthalpy flow rate of the gas turbine. If the steam turbine is operated in sliding pressure mode, and if a constant and nominal compressor inlet temperature, *TK1*, is presumed, an affine relationship between quasi-static steam turbine power output and quasi-static gas turbine power output exists, as an analysis of empirical data showed.

$$\begin{aligned} P_{ST}^{qs,mbe} = {} & P_{GT}^{Nom} \cdot k_0^{ST} - \\ & k_1^{ST} \cdot \left(P_{GT}^{Nom} - P_{GT}^{qs,mbe}|_{TK1=TK1_{Nom}} \right) \end{aligned} \tag{7}$$

As a matter of fact, variations of the compressor inlet temperature around the nominal value do only marginally impact the steam turbine power output. This circumstance is explained by the twofold and diametrical impact of the compressor inlet temperature on the steam production. With higher *TK1*, for example, an improved HRSG transformation efficiency is achieved, provided that the temperature limit of the exhaust gas is not reached. However, a rising *TK1* leads to a reduction in the exhaust enthalpy flow rate since the reduced density overcompensates the rise in mass-specific enthalpy. Hence, in total, the temperature effect on the HRSG heat transfer is offset by the variation of the enthalpy flow rate of the exhaust gas. Consequently, the influence of *TK1* on the steam turbine power output can be neglected.

If Eqn. (3) is inserted into Eqn. (7), the following correlation results for the quasi-static steam turbine power output:

$$\begin{aligned} P_{ST}^{qs,mbe} = {} & P_{GT}^{Nom} \cdot \left[k_0^{ST} - \right. \\ & \left. k_1^{ST} \cdot (1 - \gamma_{VGV}(VGV) \cdot \gamma_{TIT}(TIT)) \right]. \end{aligned} \tag{8}$$

In contrast to the compressor inlet temperature, the temperature of the steam condenser coolant media strongly impacts the steam turbine power output. Accordingly, the coefficients k_0^{ST} and k_1^{ST} of Eqn. (8) are functions of the coolant media temperature. In case of an air-cooled condenser, the ambient temperature, T_{Amb}, is used as relevant temperature, i.e.,

$$k_0^{ST} = K_0^{ST} \cdot \gamma_{CLT}(T_{Amb}) \tag{9}$$

$$k_1^{ST} = K_1^{ST} \cdot \gamma_{CLT}(T_{Amb}). \tag{10}$$

The effect of the thermal inertia of the water/steam cycle including HRSG and steam turbine is described by a second-order delay of the form

$$\Sigma_{ST}(s) = \frac{(\omega_{ST})^2}{s^2 + 2\,\zeta_{ST}\,\omega_{ST} \cdot s + (\omega_{ST})^2} \tag{11}$$

with constant parameters ζ_{ST} and ω_{ST}. The augmentation of the quasi-static relation of Eqn. (8) with this delay eventually yields the actual steam turbine power output as

$$P_{ST}^{mbe} = \Sigma_{ST}(s) \cdot P_{ST}^{qs,mbe}. \tag{12}$$

Finally, the total power output of the combined cycle system, P_{CC}^{mbe}, results as the sum of the gas turbine and steam turbine power outputs. The generator efficiency is assumed to be considered in the component contributions.

$$P_{CC}^{mbe} = P_{GT}^{mbe} + P_{ST}^{mbe} \tag{13}$$

Calibration of the Model

The mathematical model of the system was calibrated with measured and calculated performance data using least square polynomial curve fitting and nonlinear parameter identification methods in combination with multi-variable optimization techniques.

Validation of the Model

In order to validate the mathematical model against measurements, field data was acquired at the single shaft combined cycle power plant introduced further above. The selected data runs over 7 hours, contains fast as well as slow transients, and stretches over a wide load range from about 55% to 100%, relative. A comparison of experiment and model prediction is depicted in Fig. 2.

The first three subplots show the model input signals, which are the compressor inlet temperature, *TK1*, the ambient temperature, T_{Amb}, the commanded position of the variable guide vanes, *VGV*, and the commanded mixed turbine inlet temperature, *TIT*.

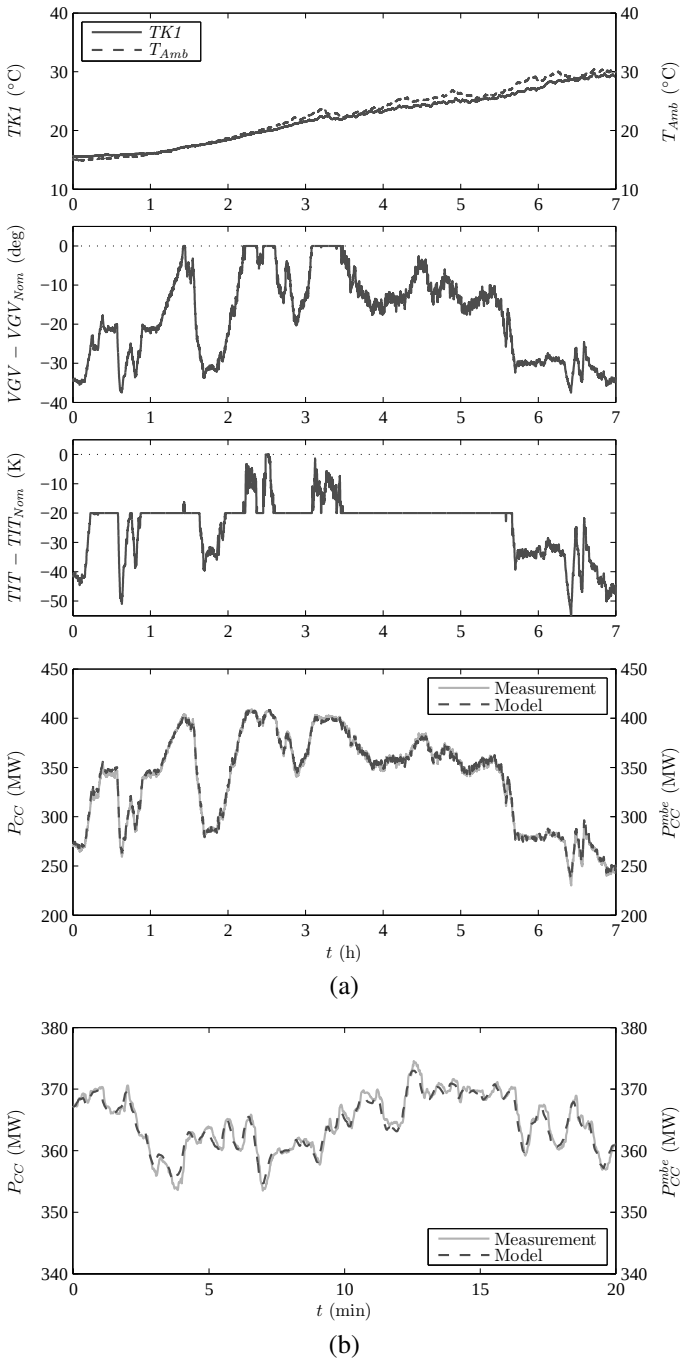

FIGURE 2. MODEL VALIDATION RESULTS.

Measurement and model prediction of the combined cycle power output are compared in the fourth subplot. As apparent from the graph, the model prediction is accurate over a wide power range. During the experiment, the deviation is within $[-7.4, 5.3]$ MW and the mean absolute error is below 1.8 MW.

The bottommost subplot of Fig. 2 shows a 20-minute excerpt of the validation results and allows an assessment of the dynamic quality of the model. Even during transients, a very good congruency between simulation and measurement is achieved.

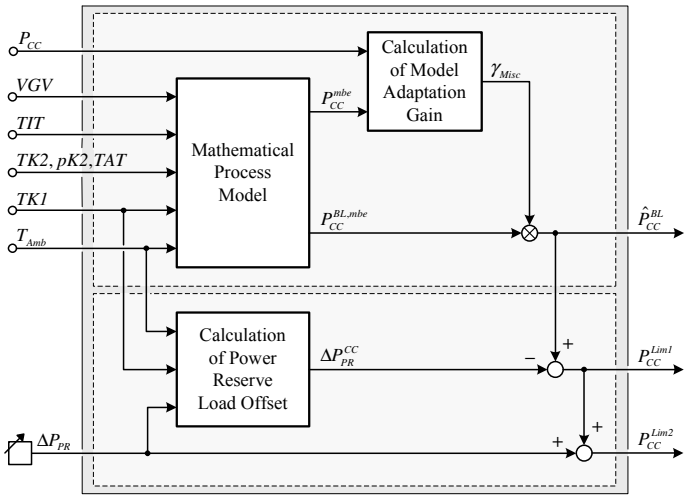

FIGURE 3. SIGNAL FLOW CHART OF THE POWER RESERVE CONTROLLER.

POWER RESERVE CONTROL CONCEPT

This section focuses on the derivation of the power reserve control concept in a first part and on the controller's integration and application in a second part. A signal flow chart of the internal structure of the power reserve controller is shown in Fig. 3. The controller features as main subsystems a module that predicts the maximum power output of the combined cycle power plant, $\hat{P}_{CC}^{BL}$, and a module that calculates the power reserve load limits, P_{CC}^{Lim1} and P_{CC}^{Lim2}, respectively. Below, the function and implementation of these two modules are detailed.

Prediction of the Maximum Power Output

The predicted maximum power output of the plant is determined in a two-step approach. Based on the mathematical model of the system, a first estimation, $P_{CC}^{BL,mbe}$, of the maximum power output is calculated. To this end, Eqn. (13) is evaluated at the predicted base load positions[3] VGV_{BL}^{mbe} and TIT_{BL}^{mbe} of the control signals VGV and TIT.

$$P_{CC}^{BL,mbe} = P_{CC}^{mbe}|_{VGV=VGV_{BL}^{mbe},TIT=TIT_{BL}^{mbe}} \tag{14}$$

[3]Positions that correspond to the maximum power output.

Principally, the actual base load positions VGV_{BL} and TIT_{BL} are given by the operating concept of the gas turbine. Though, depending on the ambient conditions, an adjustment during operation may be necessary in order to limit other process quantities, such as the turbine exhaust temperature, *TAT*, the compressor outlet temperature, *TK2*, or pressure, *pK2*. Consequently, correlations between *VGV* and *TK2*, *pK2*, *TAT*, and between *TIT* and *TAT* were derived and are used in the power reserve controller to continuously predict the actual base load positions with respect to the leading limiters.

In a subsequent step, the preliminary, model-based estimate of the maximum power output, $P_{CC}^{BL,mbe}$, is corrected for the impact of non-measured disturbances and of modeling errors to yield the prediction $\hat{P}_{CC}^{BL}$.

$$\hat{P}_{CC}^{BL} = \gamma_{Misc} \cdot P_{CC}^{BL,mbe} \tag{15}$$

In order to accomplish this model adaptation, a lumped, multiplicative correction function γ_{Misc} was introduced. The value of γ_{Misc} is unknown. However, if the correction function is assumed to be constant over the relevant power range, its value can be derived from the multiplicative model estimation error at the current operating point. This assumption is supported by the fact that both Eqn. (3) and Eqn. (8) scale with the parameter P_{GT}^{Nom}, i.e. the nominal gas turbine power output. The current multiplicative error,

$$\varepsilon_{CC} = \frac{P_{CC}}{P_{CC}^{mbe}} \tag{16}$$

is derived from the quotient of the measured power output, P_{CC}, and the power output P_{CC}^{mbe}, calculated from Eqn. (13). Aside from the relevant low-frequency errors, which originate from slow dynamics like thermal transients (i.e. heat soaking of the components), aging, dirt accumulation, or changes in the ambient conditions that are not considered in the model equations (e.g. the ambient humidity), the model-estimation error, ε_{CC}, also contains a high-frequency part. The high-frequency part may stem from deviations in the modeled power dynamics or be the result of measurement noise and must not be used to correct the estimated base load power output. Therefore, the correction function γ_{Misc} is extracted from ε_{CC} by applying a low-pass filter operation.

$$\gamma_{Misc} = \frac{1}{\tau_{Misc} \cdot s + 1} \cdot \varepsilon_{CC} \tag{17}$$

The corner frequency of the filter is defined by the application parameter τ_{Misc}.

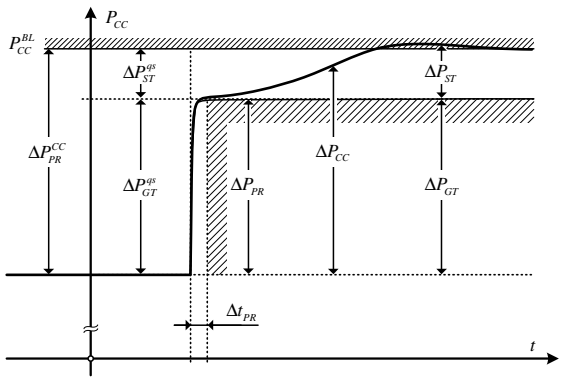

FIGURE 4. POWER RESERVE SPECIFICATION AND PLANT STEP-RESPONSE TO MAXIMUM LOAD.

Calculation of the Power Reserve Load Limits

In the second module of the power reserve controller, the predicted maximum power generation capacity, $\hat{P}_{CC}^{BL}$, is used as a reference value for the calculation of the power reserve control load limits. According to Fig. 3, the lower limit, P_{CC}^{Lim1}, is derived from this reference value by subtracting a load offset ΔP_{PR}^{CC},

$$P_{CC}^{Lim1} = \hat{P}_{CC}^{BL} - \Delta P_{PR}^{CC} \tag{18}$$

whereas the upper load limit, P_{CC}^{Lim2}, is calculated as

$$P_{CC}^{Lim2} = P_{CC}^{Lim1} + \Delta P_{PR}. \tag{19}$$

Below, the derivation of the load offset ΔP_{PR}^{CC} is elaborated. The load offset is a linear function of the specified power reserve capacity and depends on the power characteristics of the combined cycle plant. In order to explain these dependencies, a power response of the plant to a step in the load command from an initial load to maximum load is analyzed.

As shown in the illustration of Fig. 4, the change in power consists of a contribution of the gas turbine, ΔP_{GT}, and a contribution of the steam turbine, ΔP_{ST}. In sliding pressure mode, the response time of the steam turbine is slow, as it is mainly determined by the thermal inertia of the water/steam cycle. The gas turbine, however, is fast and reaches its steady-state response, ΔP_{GT}^{qs}, within seconds. Hence, reasonably fast load transients of the plant are almost exclusively provided by the gas turbine.

$$P_{CC}(t+\Delta t) - P_{CC}(t) \approx \Delta P_{GT}^{qs} \quad \forall\ \tau_{GT} \ll \Delta t \ll \frac{1}{\omega_{ST}} \tag{20}$$

In general, the response times, Δt_{PR}, specified in the grid codes for primary reserve satisfy the condition $\tau_{GT} \ll \Delta t_{PR} \ll \frac{1}{\omega_{ST}}$ of

Eqn. (20). As a consequence, the following relation of the power reserve load offsets is assumed to hold (compare also Fig. 4):

$$\frac{\Delta P_{PR}^{CC}}{\Delta P_{PR}} = \frac{\Delta P_{GT}^{qs} + \Delta P_{ST}^{qs}}{\Delta P_{GT}^{qs}}. \tag{21}$$

Equation (21) solved for the left-hand numerator yields

$$\Delta P_{PR}^{CC} = \Delta P_{PR} \cdot \left(1 + \frac{\Delta P_{ST}^{qs}}{\Delta P_{GT}^{qs}}\right). \tag{22}$$

Further, from Eqn. (3) and Eqn. (8), model-based estimates for ΔP_{GT}^{qs} and ΔP_{ST}^{qs} can be gained. If these estimates are inserted into Eqn. (22), and if common factors are canceled, the expression for the total power reserve load offset finally results as

$$\Delta P_{PR}^{CC} = \Delta P_{PR} \cdot \left(1 + K_1^{ST} \cdot \frac{\gamma_{CLT}(T_{Amb})}{\gamma_{TK1}(TK1)}\right). \tag{23}$$

Hence, for nominal T_{Amb} and $TK1$, the power reserve controller has to maintain a load offset that is $(1+K_1^{ST})$-times larger than the specified reserve capacity. It is worth to note that not the absolute power ratio P_{GT}/P_{ST} is relevant for the calculation of the offset but only the slope of the affine relation of Eqn. (7), which is significantly smaller.

Remark: Another approach to meet the power reserve specification is to set $\Delta P_{PR}^{CC} = \Delta P_{PR}$ and to compensate the dynamic lag of the steam turbine with temporary peak-firing of the gas turbine. This variation of the power reserve control concept was implemented and validated in the framework of this development project, too. However, a detailed discussion of this alternative approach would be outside the scope of this paper.

Integration and Application of the Controller

The integration of the power reserve controller into the load control of the power plant is shown in the schematic of Fig. 5. In fact, the set-up of the power reserve controller is similar to that of a state observer; based on information from its inputs and outputs, internal quantities of the system are assessed. The signals used in the power reserve controller comprise the variables *VGV* and *TIT* of the load controller, the measurable disturbance signals *TK1* and T_{Amb}, the gas turbine process measurements *TK2*, *pK2*, *TAT*, and the measured power output P_{CC}. The desired power reserve capacity ΔP_{PR} is a free parameter, which can be set by the power plant operator. Output signals of the power reserve controller are the load limits P_{CC}^{Lim1} and P_{CC}^{Lim2}, as well as the predicted maximum generation capacity, $\hat{P}_{CC}^{BL}$.

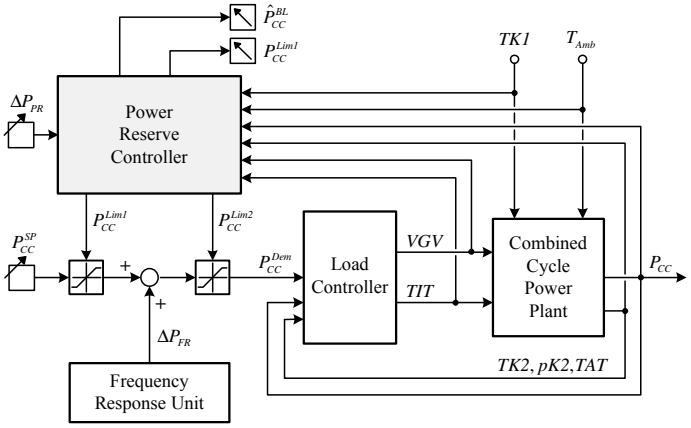

FIGURE 5. INTEGRATION OF THE POWER RESERVE CONTROLLER INTO THE LOAD CONTROL SYSTEM OF THE PLANT.

If enabled, the power reserve controller constrains the manual load set-point, P_{CC}^{SP}, at the load margin P_{CC}^{Lim1} and saves the power capacity between P_{CC}^{Lim2} and P_{CC}^{Lim1} for frequency support. The limitation at P_{CC}^{Lim2} restricts the frequency response to the declared reserve power. Eventually, the resulting load demand, P_{CC}^{Dem}, is applied as load reference value at the input of the load controller. The values of $\hat{P}_{CC}^{BL}$ and P_{CC}^{Lim1} are displayed on the operator station, in order to facilitate the dispatching of the plant.

Thanks to its model-based structure, the power reserve controller can be applied to a power plant without any commissioning effort, once calibrated for a given type of system. The only application parameter is τ_{Misc}, which defines the bandwidth of the model adaptation. Reasonable values for this parameter are in the range of 30 s to 60 s.

TEST RESULTS AND DISCUSSION

A variety of different validation tests were performed in order to demonstrate the functionality of the power reserve controller and to assess its performance. Figure 6 shows a representative extract of these field tests, which were accomplished on the single shaft combined cycle power plant introduced further above. In the graphs of Fig. 6, relevant process signals and measurements are shown over time. The time range is divided into three independent sections, A, B, and C, spanning 20 minutes each. In the uppermost subplot, the compressor inlet temperature and the ambient temperature are shown. The demanded frequency regulating power, ΔP_{FR}, is shown in the second subplot, together with the desired reserve capacity, ΔP_{PR}. In the middle subplot, the predicted maximum power output and the power reserve control load limits are shown. The load commands P_{CC}^{SP} and P_{CC}^{Dem} are depicted in the same graph. The fourth subplot

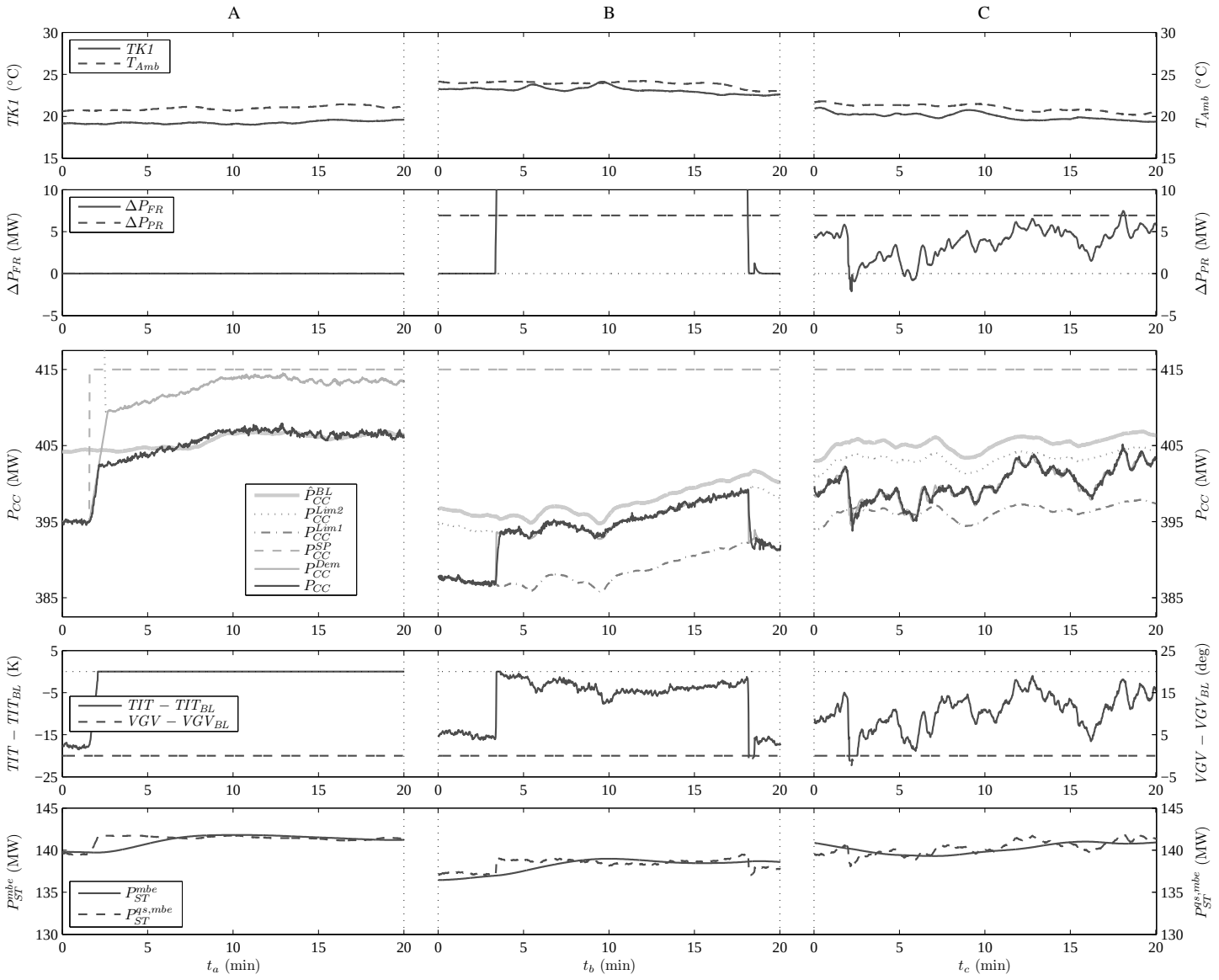

FIGURE 6. EVALUATION OF THE FUNCTIONALITY AND PERFORMANCE OF THE POWER RESERVE CONTROLLER.

contains the output signals *VGV* and *TIT* of the load controller with respect to their base load positions. During the tests shown here, the base load positions VGV_{BL} and TIT_{BL} remained constant. In the bottommost subplot, the estimated quasi-static and dynamic contributions of the steam turbine to the overall power output are shown. By comparing the quasi-static value with the dynamic value, the settling time of the system can be appraised.

The data shown in section A of Fig. 6 is used to assess the prediction accuracy of the power reserve controller. During Test A, the power reserve function was switched off (i.e., $\Delta P_{PR} = 0\,\text{MW}$) and frequency response operation was disabled. At $t_a = 1.5\,\text{min}$, the load set-point, P_{CC}^{SP}, increases from an initial value of 395 MW to 415 MW. The total load demand, P_{CC}^{Dem}, follows the step in the load set-point rate-limited and is cropped at $P_{CC} + 7\,\text{MW}$, as soon as the gas turbine reaches its base load position, i.e., at $t_a + 2\,\text{min}$, approximately. The observed power response, P_{CC}, is analogous to the one depicted in Fig. 4. About 75% of the distance to the maximum (steady-state) generation capacity are provided by the gas turbine, the remaining 25% stem from the steam turbine. The response characteristics of the steam turbine can be deduced from the bottommost subplot. Clearly, the steam turbine slightly overswings its steady-state output and

requires a settling time of 10 to 15 min. Hence, the prediction accuracy of the power reserve controller can be evaluated only at times $t_a > 15$ min, where the response of the steam turbine has settled. In this area, the predicted maximum power output, $\hat{P}_{CC}^{BL}$, coincides well with the measured power output, as apparent from the middle subplot. Actually, the mean absolute prediction error is below 0.3 MW and no prediction bias exists. Note that the increase of $\hat{P}_{CC}^{BL}$ at $t_a \approx 8$ min by approximately 2 MW is due to the influence of non-measured disturbances and captured by the model adaptation.

The results of Test B are used to demonstrate the capability of the power reserve controller to maintain in reserve a specified power capacity for frequency support. During Test B, the power reserve controller was active with a reserve capacity setting of $\Delta P_{PR} = 6.9$ MW and an assumed response time requirement of $\Delta t_{PR} = 30$ s, following the Italian Grid Code. As visible from the graph in the middle, the power reserve load limit, P_{CC}^{Lim1}, constrains the manual load set-point, which is constant at 415 MW. At $t_b \approx 3.5$ min, an artificial frequency excursion of $\Delta f = -0.35$ Hz was injected and maintained for 15 consecutive minutes. The specified reserve capacity for primary frequency response of 6.9 MW is provided within the required time as the analysis of the power response proves. Moreover, the test results validate that the power offset ΔP_{CC}^{PR} is defined properly. Indeed, the variable *TIT* touches its base load position (i.e., the gas turbine reaches maximum load) exactly at the instant when the load command P_{CC}^{Dem} saturates at the upper load limit, P_{CC}^{Lim2}. Later, when the steam turbine slowly ramps up during the period of constant frequency offset, the power output of the gas turbine automatically diminishes, as apparent from the evolution of *TIT*. Also evident from this test is the sensitivity of the maximum power output to changes in the compressor inlet temperature. Already small fluctuations in *TK1*, occurring for example at test time $t_b \approx 5$ min or $t_b \approx 10$ min, cause significant variations in the maximum power capacity, $\hat{P}_{CC}^{BL}$.

In order to demonstrate its suitability for daily operation, the power reserve controller was validated with real grid frequency in Test C. During this test, the manual load set-point was at 415 MW. A value of $P_{CC}^{SP} \geqslant P_{CC}^{Lim1}$ ensures that the power generation of the plant is maximized. The load limits P_{CC}^{Lim1} and P_{CC}^{Lim2} are continuously updated by the power reserve controller to follow the predicted maximum power output (compare middle subplot). Striking again is the impact of the ambient conditions on the maximum power output of the plant. During the 20-minute window of the test, the maximum power generation capacity varied by about 4 MW, which is of the same order of magnitude as the power demand for frequency regulation, ΔP_{FR}. In fact, the fluctuations in the grid frequency during Test C result in regulating power demands in the range of -2.1 MW to 7.5 MW, as shown in the second subplot. Even though, regulating power demands of $\Delta P_{FR} \leqslant \Delta P_{PR} = 6.9$ MW are continuously available, as the evolution of the measured power output, P_{CC}, and the evolution of *TIT* reveal. Hence, the desired power capacity is reserved from the operating range and provided for frequency support as specified.

SUMMARY AND CONCLUSIONS

With the novel method to control a power reserve margin described in this paper, an important contribution is made to optimizing the operation of a combined cycle power plant. The power reserve controller provides to the operator an accurate, real-time prediction of the plant's maximum power generation capacity and ensures by limitation of the load set-point that the operation is compliant with the grid code requirement regarding a compulsory or allocated frequency regulation reserve. Nevertheless, maximum operational flexibility is maintained as the desired reserve capacity is adjustable by the operator, and due to the fact that the power reserve controller does not substitute the normal load control but provides upper limits only.

Core of the power reserve controller is a mathematical description of the system. First step in the development of the controller was therefore the derivation, calibration, and validation of the mathematical model of the power dynamics. Key challenge during this step was to find a suitable trade-off between model complexity and resulting estimation accuracy. An increased complexity entails more calibration effort and requires more computational power during model evaluation. Beneficial in this respect was to define the model reference point at a high load. Clearly, it is most important to have a low estimation error towards maximum power. The mathematical model is applied twice in the power reserve controller. Firstly, the model equations are used to calculate a preliminary estimate of the maximum power generation capacity. In this context, the model basically has the function of correction curves. Parallel to this first use, the model is applied in the power reserve controller to determine an estimate of the current power output of the plant. This calculated value of the power output is compared with the actual, measured power output, in order to derive a model correction function. Hence, feedback information from the system is retrieved to assess the impact of miscellaneous disturbances. Subsequently, the correction function is employed to update the model-based estimate of the maximum power generation capacity. Owing to this model adaptation, the maximum power output is predicted without bias as field tests on a single shaft combined cycle power plant proved. Moreover, it was demonstrated that the controller allocates and maintains the requested power reserve capacity for frequency support with high accuracy, even under the influence of variable external disturbances.

As a matter of fact, the introduction of the power reserve controller was not only appreciated by the power plant operators

but also welcomed by the grid authorities. Indeed, the features of the controller enable the operator to maximize the power production of his plant and facilitate the optimal dispatching. Meanwhile, the controller has been implemented in six combined cycle units of different configuration and proves successful in daily commercial operation.

NOMENCLATURE

Abbreviations and Acronyms

HRSG	Heat Recovery Steam Generator
ISO	International Organization for Standardization

Symbols

f	Grid frequency (Hz)
f_{Ref}	Reference grid frequency (Hz)
Δf	Grid frequency offset (Hz)
K_{FR}	Frequency-to-power gain (MW/Hz)
K_0^{ST}	Parameter of the steam turbine model
K_1^{ST}	Parameter of the steam turbine model
k_0^{ST}	Variable coefficient of the steam turbine model
k_1^{ST}	Variable coefficient of the steam turbine model
P_{CC}	Combined cycle power output (MW)
P_{CC}^{Lim1}	Lower power reserve load limit (MW)
P_{CC}^{Lim2}	Upper power reserve load limit (MW)
$\hat{P}_{CC}^{BL}$	Predicted maximum plant power output (MW)
P_{Eff}	Effective plant power under ISO conditions (MW)
P_{GT}	Gas turbine power output (MW)
P_{ST}	Steam turbine power output (MW)
ΔP_{PR}^{CC}	Total power reserve load offset (MW)
ΔP_{FR}	Frequency regulating power (MW)
ΔP_{PR}	Desired power reserve capacity (MW)
$pK2$	Gas turbine compressor outlet pressure (Pa)
s	Complex frequency variable (s^{-1})
T_{Amb}	Ambient temperature (°C)
TAT	Gas turbine outlet temperature (K)
TIT	Commanded mixed turbine inlet temperature (K)
$TK1$	Gas turbine compressor inlet temperature (°C)
$TK2$	Gas turbine compressor outlet temperature (°C)
$t, t_{a/b/c}$	Time variable (s)
Δt_{PR}	Allowable power reserve response time (s)
VGV	Commanded variable guide vane position (deg)
Σ_{GT}	Transfer function of gas turbine power response
Σ_{ST}	Transfer function of steam turbine power response
γ_{CLT}	Variable coefficient of the steam turbine model
γ_{Misc}	System model adaptation gain
γ_{TIT}	Variable coefficient of the gas turbine model
γ_{TK1}	Variable coefficient of the gas turbine model
γ_{VGV}	Variable coefficient of the gas turbine model
ε_{CC}	Multiplicative model estimation error
ζ_{ST}	Damping coefficient of the steam turbine model
τ_{GT}	Time-constant of the gas turbine model (s)
τ_{Misc}	Time-constant of the model adaptation (s)
ω_{ST}	Eigenfrequency of the steam turbine model (s^{-1})

Subscripts and Superscripts

$_{BL}$	Base load
$_{Dem}$	Demand
$_{mbe}$	Model-based estimation
$_{Nom}$	Nominal (model reference point)
$_{qs}$	Quasi-static
$_{SP}$	Set-point

REFERENCES

[1] Terna – Rete Elettrica Nazionale, 2010. Codice di trasmissione dispacciamento, sviluppo e sicurezza della rete, ex art. 1, comma 4, DPCM 11 maggio 2004. Versione aggiornata al 12 luglio 2010.

[2] Terna – Rete Elettrica Nazionale, 2004. Code for Transmission, Dispatching, Development and Security of the Grid, as set forth in Article 1, Paragraph 4 of Prime Ministerial Decree 11 May 2004. Italian Grid Code English translation.

[3] Terna – Rete Elettrica Nazionale, 2008. Allegato A15, Partecipazione alla regolazione di frequenza e frequenza-potenza. RSPT085012DSC-PCM Rev. 01.

[4] RTE – Réseau de transport d'électricité, 2005. Référentiel technique de RTE, gestionnaire du réseau de transport d'electricité.

[5] Le ministre d'Etat, ministre de l'écologie, de l'énergie, du développement durable et de l'aménagement du territoire, France, 2008. Arrêté du 23 avril 2008 relatif aux prescriptions techniques de conception et de fonctionnement pour le raccordement au réseau public de transport d'électricité d'une installation de production d'énergie électrique. DEVE0808736A.

[6] Stevens, M., Hiddemann, M., Ruchti, C., Ruecker, F., Selby, G., Perrin, I., and Bauver, W., 2010. Alstom's KA26 Advanced Combined Cycle Power Plant Optimised for Base-Load and Cycling Duty. Power-Gen Europe, June.

[7] Parneix, S., Lindvall, K., and Philipson, S., 2007. A New Rating for the GT26 Sequential Combustion Gas Turbine. Power-Gen Middle East, January.